DETECTION OF ARTIFACTS FROM EEG DATA USING WAVELET TRANSFORM, HIGH-ORDER STATISTICS AND NEURAL NETWORKS

DAVID R. ACHANCCARAY, MARCO A. MEGGIOLARO

Laboratório de Robótica, Departamento de Engenharia Mecânica,
Pontifícia Universidade Católica do Rio de Janeiro
Rua Marquês de São Vicente, 225 – Gávea
CEP 22453-900 Rio de Janeiro - RJ - Brasil - Caixa Postal 38008
E-mails: david251@aluno.puc-rio.br, meggi@puc-rio.br

Abstract— The detection of artifacts from electroencephalogram (EEG) signals is necessary for a suitable analysis of its properties, being able to identify pathologies related with the nervous system. This paper describes the application of a method based on the decomposition of the EEG signal through the wavelet transform, extracting then high-order statistics as the entropy of Renyi and the kurtosis. With these measures, two neural networks are trained for the detection of ocular and muscular artifacts, one for each kind. The methodology is validated through experiments on an EEG implemented in this work, with hit rates of up to 94.6% for 300 trials.

Keywords— Artifact, Electroencephalogram, Wavelet Transform, Renyi's Entropy, Kurtosis, Neural Networks.

Resumo— A detecção de artefatos (*artifacts*) nos sinais de eletro-encefalograma (EEG) é necessária para uma correta análise de suas propriedades, podendo assim identificar patologias relacionadas ao sistema nervoso. Neste trabalho se descreve um método baseado na decomposição do sinal EEG mediante a transformada *wavelet*, extraindo logo medidas estatísticas de alta ordem, como a entropia de Renyi e a curtose. Com estas medidas, duas redes neurais foram treinadas para a detecção de artefatos oculares e musculares, uma para cada tipo. A metodologia é validada através de experimentos em um EEG implementado em este trabalho, obtendo taxas de acerto de até 94,6% para 300 amostras.

Palavras-chave— Artefato, Eletro-encefalograma, Transformada *Wavelet*, Entropia de Renyi, Curtose, Redes Neurais.

1 Introduction

Electroencephalography (EEG) is the neurophysiologic measurement of the electrical activity of the brain recorded through electrodes placed on the scalp (Inuso et al., 2007). The signal is the endogenous brain activity measured as voltage changes at the scalp, while a perturbation is any voltage change generated by other sources. The perturbation sources include: electromagnetic interferences, eye blinks, eye movements, and muscular activity (particularly head muscles). In this paper, the term noise is used for external perturbations (e.g. power line noise) and artifact for subject related perturbations (e.g. muscular and eye movement artifacts).

Eye blink artifacts are very common in EEG data; they produce low-frequency high-amplitude signals that can be quite greater than EEG signals of interest. Indeed, while regular EEG amplitudes are in the range of −50 to 50 micro volts, eye blink artifacts have amplitudes up to 100 micro volts (Garcia, 2004).

Eye movement artifacts are caused by their orientation of the retinocorneal dipole. They are recognized by their quasi square shape and their amplitude in the same range of regular EEG (Overton & Shagass, 1969).

Eye blink and eye movement artifacts (henceforth called ocular artifacts) are mainly reflected at frontal sites (e.g. electrodes Fp1 and Fp2, denominated according to the International System 10-20, see Garcia, 2004). However, they can corrupt data on all electrodes, even those at the back of the head.

Muscular movement artifacts (muscular artifacts) can be caused by activity in different muscle groups. However, the activity in neck and facial muscles has more influence in EEG recordings. Muscular artifacts are characterized by their wide frequency content. Depending on the location of the source muscles, they can be distributed across different sets of electrodes. They mainly appear in temporal and parietal electrodes (Garcia, 2004).

Even if muscular and ocular artifacts are not correlated with the mental activities that the subject is executing, they make it difficult to extract useful information from the data.

Furthermore, artifacts can lead to erroneous conclusions about the Brain Computer Interface (BCI) controlling performance of a subject. Indeed, the BCI could be responding to muscular or ocular activity instead of genuine EEG (Garcia, 2004). To prevent these errors, this paper describes the application of a method based in the decomposition of the EEG signal through the wavelet transform, until achieving the frequency ranges of the brainwaves. High-order statistics is then extracted as the entropy of Renyi and the kurtosis in the wavelet coefficients that evidence the existence of artifacts. With these measures, two neural networks were trained for the detection of ocular and muscular artifacts, one for each kind.

The detection system was tested with two kinds of neural networks as classifiers, multilayer perceptron (MLP) and radial basis function (RBF).

2 Wavelet Analysis

Wavelet transform is rapidly surfacing in fields as diverse as telecommunications and biology. Because of their suitability to analyze nonstationary signals, those whose statistical properties change over time, they have become a powerful alternative to Fourier methods in many medical applications, where such signals abound. In addition to helping in the recognition and detection of key diagnostic features, they provide a powerful means for compressing medical images with little loss of valuable information (Akay, 1997)..

The familiar Fourier transform expands time-domain signals onto orthogonal basis functions (sine and cosine waves), thereby revealing the frequency content of the signals. But this method can not localize the observed frequency components in time. It is therefore best suited to describe and analyze stationary signals (Akay, 1997).

Most biomedical signals, however, do not tend to be stationary. On the contrary, they typically have highly complex time-frequency components closely spaced in time, accompanied by long-lasting, low-frequency components closely spaced in frequency. Any appropriate analysis method for dealing with them should therefore exhibit good frequency resolution with fine time resolution, the first to localize the low-frequency components, and the second to resolve the high-frequency components (Akay, 1997).

An alternative way to analyze nonstationary biomedical signals is to expand them onto basis functions created by expanding, contracting, and shifting a single prototype function, specifically selected for the signal under consideration. This wavelet method acts as a sort of mathematical microscope through which different parts of the signal may be examined by adjusting the focus. In wavelet parlance, the prototype function is known as the "analyzing wavelet" or "mother wavelet" of the signal.

Wavelet transforms can provide both very good time resolution at high frequencies and good frequency resolution at low frequencies. Interestingly, they can do so even in the absence of continuous time and frequency parameter information, thanks to the redundancies inherent in continuous wavelet signal representations. In fact, in practical applications, to reduce memory requirements and speed up numerical computation, it is usually desirable to eliminate much of this redundancy, usually by sampling the time and frequency parameters on a dyadic form (basis 2, the widely used choice) in the time-frequency plane (Akay, 1997)..

Even without the efficiencies of sampling, their excellent combination of time and frequency resolution makes wavelets potentially invaluable in numerous applications, many of which fall into the realm of medical research and diagnostics. Among them, it may be found the early discovery of precursors of heart disease, studies of fetal breathing, the extraction of speech from background noise in digital hearing aids, the detection of breast cancer, and medical image compression (Akay, 1997).

The key feature of wavelets is the time-frequency localization. It means that most of the energy of the wavelet is restricted to a finite time interval (Jahankhani et al., 2006).

The wavelet technique applied to the EEG signal will reveal features related to the transient nature of the signal. All wavelet transforms can be specified in terms of a low-pass filter *g*, which satisfies the standard quadrature mirror filter condition

$$G(z)G(z^{-1}) + G(-z)G(-z^{-1}) = 1 \qquad (1)$$

where $G(z)$ denotes the z-transform of the filter *g*. Its complementary high-pass filter can be defined as

$$H(z) = zG(-z^{-1}) \qquad (2)$$

A sequence of filters with increasing length can be obtained

$$\begin{aligned} G_{i+1}(z) &= G(z^{2^i})G_i(z), \\ H_{i+1}(z) &= H(z^{2^i})G_i(z), \quad i = 0,...,l-1 \end{aligned} \qquad (3)$$

with the initial condition $G_0(z) = 1$. It is expressed as a two-scale relation in time domain

$$g_{i+1}(k) = [g]_{\uparrow 2^i} g_i(k), h_{i+1}(k) = [h]_{\uparrow 2^i} g_i(k) \quad (4)$$

where the subscript $[.]_{\uparrow m}$ indicates the up-sampling by a factor of *m* and *k* is the equally sampled discrete time (Jahankhani et al., 2006).

The procedure of the discrete wavelet transform (DWT) is schematically shown in Figure 1. Each stage of this scheme consists of two digital filters and two down-samplers by 2. The first filter *h*[.] is the discrete mother wavelet, high-pass in nature, and the second, *g*[.], is its mirror version, low-pass in nature.

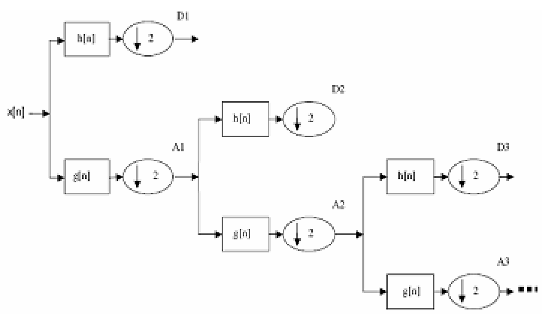

Figure 1. Sub-band decomposition of DWT implementation.

The down-sampled outputs of first high-pass and low-pass filters provide the detail D1 and the approximation A1, respectively. The first approximation A1 is further decomposed and this process is continued as shown in Figure 1 (Jahankhani et al., 2006).

In this work, an EEG was implemented having some problems with the noise, these problems are treated digitally. The EEG signal is previously filtered to guarantee that only has frequency components in the EEG band through a low-pass Butterworth filter of order 4, with a frequency cut of 100 Hz, and then through a Filter Notch centered in the frequency of 60 Hz. The EEG signal is decomposed through the DWT until achieving the frequency ranges of the brainwaves. The signal decomposition is shown in Figure 2, the decomposition begin in 500 Hz due to the sample rate of 1 KHz.

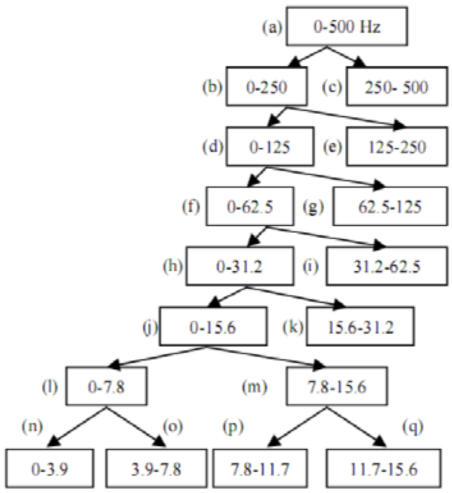

Figure 2. Decomposition of the frequency ranges.

The DWT is applied in seven levels, according to Figure 2, in order to approximately form the four principal frequency ranges of the brainwaves (Garcia, 2004):

- Delta Band [0 – 4 Hz]: (n).
- Theta Band [4 – 8 Hz]: (o).
- Beta Band [13 – 30 Hz]: (q) and (k).
- Alpha Band [8 – 13 Hz]: (p).

Ocular artifacts have large amplitudes. Their spectral content is mainly concentrated in the theta band. They are more prominent at frontal pole electrodes, i.e. Fp1 and Fp2 (Garcia, 2004).

Muscular artifacts have amplitudes in the order of that of regular EEG, but their spectral content is concentrated in the beta band. These artifacts are more noticeable in central temporal and parietal electrodes, i.e. electrodes T3, T4, T5, P3, P4 and T6, denominated according to the International System 10-20 (Garcia, 2004).

For our analysis, the beta and theta bands are processed to obtain their respective wavelet coefficients using the electrodes Fp1, Fp2, P3 and P4, see Figure 3.

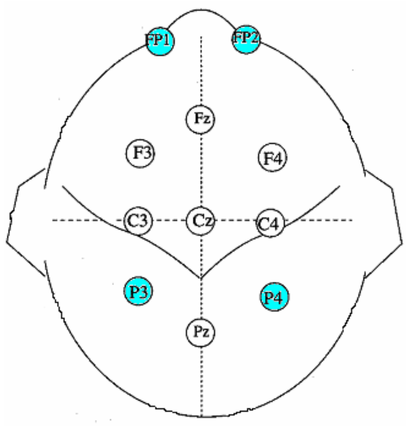

Figure 3. Electrodes position according to the International System 10-20.

3 Feature Extraction

The feature extraction is done through high-order statistics such as the entropy of Renyi and the kurtosis.

Wavelet coefficients for artifactual activity are supposed to be “odd” with respect to other ones when an unexpected event occurs and involves its frequency range, or when it carries information about a noisy background activity. Thus, a measure of randomness might help to detect them. EEG artifacts such as eye blinks and heartbeat are typically characterized by a peaky distribution and could be detected by a measure of peakyness (Inuso et al., 2007).

The parameters that can measure the randomness and the peakyness are entropy and kurtosis, respectively (Delorme et al., 2005).

3.1 Kurtosis.

Given a scalar random variable x, kurtosis has the following expression:

$$k = m_4 - 3m_2^{\ 2} \tag{5}$$

$$m_n = E\{(x - m_1)^n\} \tag{6}$$

where m_n is the n-order central moment of the variable and m_1 is its mean.

If the kurtosis is highly positive, the activity value distribution is highly peaked (usually around zero) with a sparse appearance of extreme values, and the identified data is likely to contain an artifact (Ghandeharion & Erfanian, 2004).

3.2 Renyi's Entropy.

The definition of the Renyi's entropy is shown in Equation (7), where α (α ≥ 1) is the order of the entropy. Equations (8-9) come from the application of the kernel estimators. The order of the entropy is set at 2, in order to equally emphasize the sub-

Gaussian and the super-Gaussian components (Erdogmus et al., 2002).

$$H_{R_\alpha}(X) = \frac{1}{1-\alpha} \log \sum_i P^\alpha (X = a_i) \quad (7)$$

$$H_{R_\alpha}(x) = \frac{1}{1-\alpha} \log \int_{-\infty}^{\infty} \rho_X{}^\alpha (x) dx \quad (8)$$

$$H_{R_\alpha}(X) = \frac{1}{1-\alpha} \log \{ \frac{1}{N^\alpha} \sum_j [\sum_i k_\sigma (x_j - x_i)^{\alpha-1}]\} \quad (9)$$

Entropy can be interpreted as a measure of randomness.

Before computing the entropy and the kurtosis of the wavelet coefficients, they are normalized with zero-mean and unit-variance. After computing the statistic data, it is observed that a simple threshold is not enough to discriminate the occurrence of artifacts. Thereby, a few measurements are selected below as patterns for training a neural network.

4 Detection of Artifacts

The detection system is tested with two kinds of neural networks as classifiers: multilayer perceptron and radial basis function. The detection system consists of two neural networks, of the same class, joined through a logic operation OR.

The MLP has the ability to learn and generalize with smaller training set requirements. It has a fast operation, ease of implementation and therefore it is the most commonly used neural network architecture. It has been adapted to discriminate between the occurrence and the non occurrence of artifacts. The classic gradient descending learning scheme is used here for the training of this particular network.

The second kind of classifier is an RBF scheme. The RBF network is rapidly trained; it is usually faster than MLP, while exhibiting none of its training pathologies such as paralysis or local minima problems (Jahankhani, 2006).

After of analyzing the variations of the statistics, the detection of ocular artifacts is achieved using the wavelet coefficient kurtosis of the four electrodes (Fp1, Fp2, P3 and P4) in the frequency ranges beta (o) and theta (k); while the detection of muscular artifacts is achieved using the wavelet coefficient entropy and kurtosis of three electrodes (Fp1, Fp2 and P4) in the frequency range theta (k), see Figure 2.

The experience is performed considering 300 trials: 100 trials without artifacts, 100 trials with ocular artifacts, and 100 trials with muscular artifacts. To produce artifacts, the user was asked to generate artifacts voluntarily; and for the trials without artifacts, the user stay in relax condition with the open eyes.

The training of the neural networks is done as follows. Neural network 1 (net1) is trained using 100 trials without artifacts, and 100 trials with ocular artifacts, taking 20% of the trials for the test of the neural network. Neural network 2 (net2) is trained in the same way, however using muscular instead of ocular artifacts.

5 Results

The union of the neural networks (netf), made through a logic operation OR as discussed before, is tested for the total of the trials. The results of the test of the neural networks are shown in Tables 1 and 2.

Tables 3 and 4 show the confusion matrices of the detection system using MLP and RBF respectively.

The tables show that the approach for the processing of the EEG signals and for the detection of the artifacts is suitable. The better hit rate is 94.6%, obtained by the detection system using RBF classifiers, closely followed by the hit rate using MLP classifiers, with 94.3%. This last network can increase the hit rate to an even higher value depending on the training. On the other hand, the RBF classifiers would maintain the same hit rate.

Table 1. Test of the MLP neural networks (individually and united). C: Correct. I: Incorrect.

	C	I	Total	Hit Rate (%)
net1	35	5	40	87.5
net2	27	13	40	67.5
netf	283	17	300	94.3

Table 2. Test of the RBF neural networks (individually and united). C: Correct. I: Incorrect.

	C	I	Total	Hit Rate (%)
net1	24	16	40	60.0
net2	27	13	40	67.5
netf	284	16	300	94.6

Table 3. Confusion Matrix of the Classification with MLP neural networks. S: Signal without artifact. SA: Signal with artifact.

	S	SA
S	87	13
SA	4	196

Table 4. Confusion Matrix of the Classification with RBF neural networks. S: Signal without artifact. SA: Signal with artifact.

	S	SA
S	88	12
SA	4	196

6 Conclusions

In this work, a technique was used to detect artifacts using only four electrodes Fp1, Fp2, P3 and P4, and trials of 2000 samples recorded during two seconds. In comparison with other techniques from the literature, the union of neural networks through a logic operation resulted in a considerable increase in performance. The specialization of the neural networks demonstrates that the system could increase even more its hit rate. Thereby, this method leaves the EEG signals free of artifacts for a more elaborated analysis.

Others techniques as independent component analysis (ICA) (Delorme et al., 2005) were approached to prepare the data of the EEG signal to discriminate the artifacts occurrence. The high order statistics and wavelet transform were used to determine thresholds to detect the presence of artifacts; but simulating the behavior of these (Inuso et al., 2007).

The inconvenient of several methods approached to detect artifacts is that they do not follow a pattern; from which can be compared between them.

References

Akay, M. (1997). Wavelets applications in medicine. *Spectrum*, May 1997, pp. 50-57.

Delorme, A., Jung, T., Sejnowski, T., Makeig, S. (2005). Improved rejection of artifacts from EEG data using high-order statistics and independent component analysis. *Neuroimage*.

Erdogmus, D., Hild, K. E. II and Principe, J. C. (2002). Blind source separation using Renyis marginal entropies. *Neurocomputing,* v. 49, pp. 25-38.

Garcia, G. N., (2004). Direct brain-computer communication through scalp recorded EEG signals, *Doctor's thesis, Department of Electricity, Ecole Polytechnique Fédérale de Lausanne,* Lausanne.

Ghandeharion H. and Erfanian A. (2004). A fully automatic method for ocular artifact suppression from EEG data using wavelet transform and independent component analysis. P*roceedings of the 28th IEEE EMBS Annual Internatonal Conference,* pp. 5265-5268.

Inuso, G., La Floresta F., Mammone, Nadia, and Morabito, F. C. (2007). Brain activity investigation by EEG processing: wavelet analysis, kurtosis and Renyi's entropy for Artifact Detection, *Proceedings of the 2007 International Conference on Information Acquisition,* Jeju City, pp. 195–200.

Jahankhani, P., Kodogiannis, V. and Revett, K. (2006). EEG signal classification using wavelet feature extraction and neural networks. *Jhon Vincent Atanasoff 2006 International Symposium on Modern Computing,* pp. 120-124.

Overton D. A. and C. Shagass (1969). Distribution of eye movement and eye blink potentials over the scalp, *Electroencephalography and Clinical Neurophysiolog*y, n. 27, pp. 546.